THE JOURNAL OF BIOLOGICAL CHEMISTRY VOL. 283, NO. 47, pp. 32848–32859, November 21, 2008

Crystal Structures of the Choline/Acetylcholine Substrate-binding Protein ChoX from *Sinorhizobium meliloti* in the Liganded and Unliganded-Closed States*

Received for publication, August 5, 2008, and in revised form, August 25, 2008 Published, JBC Papers in Press, September 8, 2008, DOI 10.1074/jbc.M806021200

Christine Oswald[‡], Sander H. J. Smits[‡], Marina Höing[§1], Linda Sohn-Bösser[§], Laurence Dupont[¶], Daniel Le Rudulier[¶], Lutz Schmitt[‡2], and Erhard Bremer[§]

From the [‡]Institute of Biochemistry, Heinrich Heine University Duesseldorf, Universitaetsstrasse 1, 40225 Duesseldorf, Germany, [§]Laboratory for Microbiology, Department of Biology, Philipps University Marburg, Karl-von-Frisch Strasse, 35032 Marburg, Germany, and [¶]Unité Interactions Plantes-Microorganismes et Santé Végétale, UMR6192 CNRS-Institut National de la Recherche Agronomique (INRA)-Université de Nice Sophia Antipolis, Centre INRA Agrobiotech, Sophia Antipolis Cedex, France

The ATP-binding cassette transporter ChoVWX is one of several choline import systems operating in *Sinorhizobium meliloti*. Here fluorescence-based ligand binding assays were used to quantitate substrate binding by the periplasmic ligand-binding protein ChoX. These data confirmed that ChoX recognizes choline and acetylcholine with high and medium affinity, respectively. We also report the crystal structures of ChoX in complex with either choline or acetylcholine. These structural investigations revealed an architecture of the ChoX binding pocket and mode of substrate binding similar to that reported previously for several compatible solute-binding proteins. Additionally the ChoX-acetylcholine complex permitted a detailed structural comparison with the carbamylcholine-binding site of the acetylcholine-binding protein from the mollusc *Lymnaea stagnalis*. In addition to the two liganded structures of ChoX, we were also able to solve the crystal structure of ChoX in a closed, substrate-free conformation that revealed an architecture of the ligand-binding site that is superimposable to the closed, ligand-bound form of ChoX. This structure is only the second of its kind and raises the important question of how ATP-binding cassette transporters are capable of distinguishing liganded and unliganded-closed states of the binding protein.

The quaternary amine choline is commonly found in soil and the rhizosphere (1) where it can be utilized by microorganisms for various physiological processes. The plant root-associated soil bacterium *Sinorhizobium meliloti*, which is involved in the fixation of nitrogen and its delivery to its host plant *Medicago sativa* (2), uses choline as the sole carbon and nitrogen source (1). Furthermore it also uses choline as the precursor for the synthesis of the osmoprotectant glycine betaine (3, 4). Besides *S. meliloti* forms phosphatidylcholine, a membrane lipid normally found in low amounts in prokaryotes, from choline and CDP-diacylglyceride by the phosphatidylcholine synthase (5, 6). In light of these diverse physiological functions of choline in *S. meliloti*, this soil bacterium has developed several systems for choline uptake (7). One of these is the choline-inducible transport system ChoVWX (8), a member of the superfamily of microbial substrate-binding protein (SBP)[3]-dependent ABC transporters (9). In the case of the ABC importer ChoVWX from *S. meliloti*, ChoV serves as the nucleotide-binding domain that provides energy for the transport process via ATP hydrolysis, ChoW is the integral cytoplasmic membrane protein that forms the substrate translocation pathway, and ChoX is the substrate-binding protein located in the periplasm (8). Binding assays with ^{14}C-labeled choline and competition studies with compounds structurally related to choline have demonstrated that ChoX recognizes both choline (K_D = 2.7 μM) and acetylcholine (K_D = 145 μM) as ligands (8).

It is generally thought that the substrate-binding protein confers specificity and directionality to a given microbial binding protein-dependent ABC transport system (9, 10). These binding proteins are either located in the periplasmic space of Gram-negative bacteria or are anchored at the cell surface in Gram-positive bacteria or archaea. The binding protein serves to capture the ligand with high affinity (mostly in the nM or low μM range) from substrate-depleted environments and delivers the ligand to the transmembrane domains of the ABC system. Upon ATP binding and hydrolysis by the cytoplasmically located nucleotide-binding domain, the substrate is released into the translocation complex and finally imported into the cell (9, 10). Recently structural insight into the interactions of substrate-binding proteins with the cognate transmembrane domains of bacterial ABC transporters have been obtained for

* This work was supported in part by grants from the University of Duesseldorf (to L. S.) and the Deutsche Forschungsgemeinschaft through SFB 395, the Fonds der chemischen Industrie, and the Max Planck Institute for terrestrial Microbiology (Marburg, Germany) (to E. B.). The costs of publication of this article were defrayed in part by the payment of page charges. This article must therefore be hereby marked "*advertisement*" in accordance with 18 U.S.C. Section 1734 solely to indicate this fact.

The atomic coordinates and structure factors (codes 2REG, 2RF1, and 2RIN) have been deposited in the Protein Data Bank, Research Collaboratory for Structural Bioinformatics, Rutgers University, New Brunswick, NJ (http://www.rcsb.org/).

[1] Recipient of a Ph.D. fellowship from the International Max Planck Research School for Environmental, Cellular and Molecular Microbiology (Marburg, Germany).

[2] To whom correspondence should be addressed. Tel.: 49-211-81-10773; Fax: 49-211-81-15310; E-mail: lutz.schmitt@uni-duesseldorf.de.

[3] The abbreviations used are: SBP, substrate-binding protein; ABC, ATP-binding cassette; ACh, acetylcholine; Se-Met, selenomethionine; r.m.s.d., root mean square deviation; AChBP, acetylcholine-binding protein; GGBP, galactose/glucose-binding protein; NCBI, National Center for Biotechnology Information; BLAST, Basic Local Alignment Search Tool.

the putative molybdate importer ModABC from the archaeon *Archaeoglobus fulgidus* (11), the vitamin B_{12} importer BtuCDF (12) and the maltose importer MalKEFG from *Escherichia coli* (13).

Structural studies of a substantial number of bacterial substrate-binding proteins revealed a general bilobal fold for this class of proteins (9, 14, 15). The substrate-binding site lies within a cleft that is dynamically formed by the two domains of the SBP upon capturing of the substrate. The two lobes of the binding protein are subjected to an opening and closing movement relative to each other, thereby opening and closing the path to the substrate-binding site (15). A flexible linker connects the two domains and permits a hinge-bending movement (16) that leads to rigid-body motions conducted by both domains of the SBP. The ligand is thereby trapped deep within the binding protein and thus is largely occluded from the surrounding solvent (9, 14, 15).

In the absence of substrate, the two physical states of the binding protein, unliganded-open and unliganded-closed, are in equilibrium, and it is thought that the binding of the ligand shifts this ratio toward the liganded-closed state (9, 14, 15). Crystal structures of SBPs both in the open (without a ligand) and the closed (with a ligand) forms have been determined for a substantial number of microbial SBPs (9, 14, 15). In addition, crystal structures of the ribose and allose sugar-binding proteins from *E. coli* in various unliganded forms have been analyzed that allow tracing the path of the conformational changes occurring in the binding protein during ligand capturing and the formation of the liganded, closed structure (17, 18). Remarkably it has also been possible, although for only a single SBP, to elucidate the crystal structure of the unliganded-closed state (19). Taken together, these structural and other biochemical and biophysical data have given considerable support to the so-called "Venus fly trap mechanism" of substrate binding by SBPs (14, 20).

Because no crystal structures of substrate-binding proteins with either choline or acetylcholine as ligand are available, we set out to determine the structure of the *S. meliloti* ChoX protein in complex with its substrates. This structural analysis revealed a ligand binding pocket and mode of substrate binding similar to that previously reported for several microbial glycine betaine/proline betaine-compatible solute-binding proteins (21–24). Furthermore we were able to solve the crystal structure of ChoX in a substrate-free closed conformation with an architecture of the ligand-binding site that is superimposable for the closed ligand-bound and closed-unliganded forms of ChoX. This obviously raises the question of how the cognate transporter is capable to distinguish between these two states of the SBP.

EXPERIMENTAL PROCEDURES

Growth Studies of S. meliloti Strain 2011 on Different Carbon Sources—A preculture of *S. meliloti* strain 2011 grown in LB media supplemented with 2.5 mM $MgSO_4$ and 2.5 mM $CaCl_2$ was harvested and inoculated in M9 minimal medium (25) supplemented with either the sugar mannitol or the trimethylammonium compounds choline or ACh (0.2% (w/v)) as the sole carbon sources. Growth behavior of the *S. meliloti* strain 2011 in the presence of the different carbon sources was followed by measuring the absorbance (A_{600}) over time.

Protein Expression and Purification—Expression and purification of ChoX were performed as described previously (8). In brief, *choX* was overexpressed in the *E. coli* strain BL21(pLysS) (Stratagene, La Jolla, CA) using the pET20b vector-derived expression plasmid pETNx (8). Cells were grown in minimal medium with glucose as the carbon source to avoid the capturing of chemically undefined ligands by ChoX from components of rich medium. 5 liters of minimal medium in a 10-liter flask was inoculated from an overnight-grown preculture of strain BL21(pLysS pETNx) to an absorbance (A_{578}) of 0.1, and the cells were grown with rapid stirring of the culture at 37 °C. Expression of the pETNx encoded *choX* gene was induced by the addition of isopropyl 1-thio-β-D-galactopyranoside (final concentration, 0.5 mM) when the culture reached an A_{578} of about 0.5. After *choX* induction, the bacterial culture was grown for an additional 2 h, and the cells were then harvested by centrifugation. The *choX* gene encodes a protein with a signal sequence to properly target it into the periplasm of the *E. coli* host strain. To release the periplasmically located proteins, the ChoX-overproducing cells were subjected to a rapid osmotic shock by resuspending them in ice-cold buffer (50 mM NaH_2PO_4, 300 mM NaCl, 10 mM imidazole, pH 8.0, 500 mM sucrose) followed by incubation on ice for 30 min. After ultracentrifugation, the supernatant was applied on a nickel-nitrilotriacetic acid column for affinity purification of the His-tagged ChoX protein. Buffer A (50 mM NaH_2PO_4, 300 mM NaCl, 10 mM imidazole, pH 8.0) was used for washing of the columns. His-tagged ChoX protein retained by the nickel-nitrilotriacetic acid column was eluted from the affinity matrix by using a gradient from 10 to 250 mM imidazole, utilizing Buffer A and Buffer B (50 mM NaH_2PO_4, 300 mM NaCl, 250 mM imidazole, pH 8.0). To exchange the buffer of the eluted ChoX protein-containing fractions, the protein was dialyzed at 4 °C against 5 liters of 10 mM Tris/HCl, pH 7.0 buffer for crystallization experiments or against 5 liters of 10 mM Tris/HCl, pH 7.4, 200 mM NaCl buffer for substrate binding assays using an intrinsic tryptophan fluorescence-based assay. To obtain selenomethionine (Se-Met)-substituted ChoX protein, cells of strain BL21(pLysS pETNx) were grown in glucose minimal medium that was supplemented with 100 mg each of Lys, Phe, and Thr (10 mg/ml) and 50 mg each of Ile, Leu, and Val (5 mg/ml) just prior to the induction of *choX* expression to inhibit methionine biosynthesis. Incorporation of Se-Met was achieved by the subsequent addition of 60 mg of L-Se-Met (6 mg/ml). The Se-Met-substituted ChoX protein was purified as described above for the unmodified ChoX protein and used after dialysis for crystallization trials.

Ligand Binding Experiments—The affinity of the purified ChoX protein for the different ligands was determined by intrinsic tryptophan fluorescence. Upon binding of the ligand to the tryptophan/tyrosine box (see Fig. 4), the intrinsic fluorescence of tryptophan is quenched. The excitation wavelength was set to 295 nm, and fluorescence was monitored from 310 to 370 nm using a FluoroMax (Jobin Yvon, Horiba, Edison, NJ) with slit widths of 3 nm at 22 ± 1 °C. Different amounts of ligands in 200 mM NaCl, 10 mM Tris/HCl, pH 7.4 (from 0.5, 2.5,

5, 50, 100, and 500 mM stocks) were titrated to ChoX (600 nM) in 200 mM NaCl, 10 mM Tris/HCl, pH 7.4. To account for background fluorescence, spectra with and without protein were subtracted from each other. All data were averaged from two independent measurements and analyzed according to Equation 1 in the case of acetylcholine and glycine betaine.

$$\%\ \text{quenching} = \frac{F_{q,\max} \times [S]}{K_D + [S]} \qquad \text{(Eq. 1)}$$

Here $F_{q,\max}$ is the maximal quenching observed, [S] is the substrate concentration, and K_D is the affinity constant of the ChoX-choline complex. In the case of choline, spectra were background-corrected and analyzed according to Equation 2, which corrects for the high protein concentrations used (26). T represents the protein concentration, K_d represents the dissociation constant, $B_{\max}$ represents the maximum amount of bound substrate, and [S] represents the substrate concentration.

$$F/F_0 = (K_d + T + [S]) - \sqrt{(K_d + T + [S])^2 - 4T[S]}/(2/TB_{\max}) \qquad \text{(Eq. 2)}$$

Crystallization of ChoX in the Presence and Absence of a Ligand—Purified ChoX protein (10 mg/ml) was mixed with 1 mM choline and incubated on ice for at least 30 min prior to crystallization. Crystals were obtained using the hanging drop vapor diffusion method at 293 K against a reservoir solution of 100 mM sodium acetate, pH 4.8–5.0, 15–25% polyethylene glycol 3350. Protein was mixed with mother liquor 1:1 to a final volume of 2 μl. Crystals of wild type as well as the Se-Met-incorporated ChoX protein with choline were obtained after 4 weeks and had a size of 50 × 20 × 200 μm. To obtain crystals in the unliganded state, streak seeding at 277 K, utilizing ChoX-choline microcrystals, was established (27). Crystals grew in less than 1 day and were immediately flash frozen in liquid nitrogen. In all cases the mother liquor supplemented with 20–25% ethylene glycerol was used as cryoprotectant.

Data Collection, Refinement, and Structure Analysis—All data sets were collected at the Max Planck beam line BW6 or the European Molecular Biology Laboratory beam line BW7A (Deutsches Elektronen Synchrotron, Hamburg, Germany). Data statistics are given in Table 1. A three-wavelength anomalous dispersion experiment using an Se-Met-incorporated ChoX-choline crystal was collected at a resolution of 2.9 Å. All data sets were processed with DENZO (28) or XDS (29). To obtain initial phases, SOLVE/RESOLVE was utilized (30). Eleven of the 14 Se-Met sites present in ChoX were detected leading to a mean figure of merit of 0.49. The model was further refined using REFMAC5 (31) with additional rounds of manual rebuilding using COOT (32), resulting in a model for one of the two monomers present in the asymmetric unit. This model was used as a template for the high resolution data set of ChoX-choline at 1.9 Å utilizing the molecular replacement program MOLREP (33), resulting in two monomers in the asymmetric unit. The same model was used as a template for molecular replacement for the ChoX unliganded-closed (2.0 Å) and ChoX-acetylcholine (1.8 Å) structures. For the last two data sets

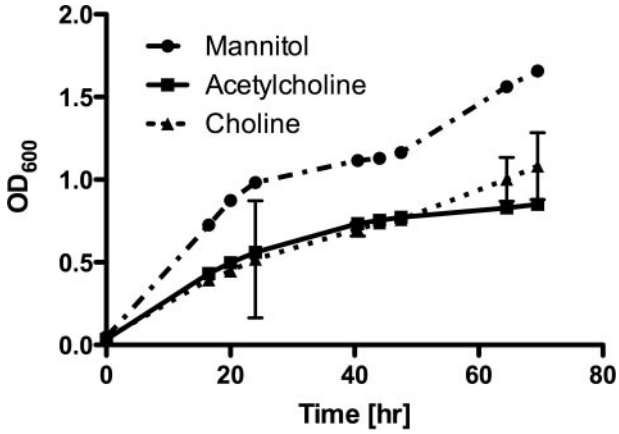

FIGURE 1. **Growth curves of *S. meliloti* strain 2011 on different carbon sources (mannitol, *dashed-dotted line*; choline, *dotted line*; and acetylcholine, *solid line*).** Data points are given as mean ± S.D. of two independent experiments.

the algorithm of Padilla and Yeates revealed a perfect twin (twinning factor $\alpha > 0.479$) (55). These structures were further refined using SHELXL97–2 (34) with (h,−k,−l) as twinning operator. Water molecules were first detected using ARP/wARP (35) (threshold of 3.2σ) and further manually checked. Data set and refinement statistics are listed in Table 1. As analyzed with Molprobity (36), the Ramachandran plot of the structures of ChoX-choline, ChoX-acetylcholine, and ChoX in the unliganded-closed state show none, 0.3%, and 0.3% of the residues in the disallowed regions, respectively. However, these residues are taking part in crystal contacts, explaining this rather high percentage. Figures of protein molecules were created using PyMol.

Data Bank Searches and Sequence Alignments—Protein homologues of the *S. meliloti* ChoX protein were searched via the Web server of the National Center for Biotechnology Information (NCBI BLAST) (37). Sequence alignments of ChoX-related proteins were performed using ClustalW (38) as implemented in the Vector NTI 10.0 software package (Invitrogen). An alignment of the ChoX protein from *S. meliloti* with the OpuAC protein from *Bacillus subtilis* (Fig. 7) was performed by applying an "in-domain" cut in the OpuAC sequence between amino acid residues 168 and 169 and by inverting the N-terminal and C-terminal portions of the OpuAC protein for the sequence alignment to ChoX as described previously (24, 39).

Protein Data Bank Accession Numbers—Coordinates and structure factors for the various crystal structures of ChoX described in this study have been deposited in the Protein Data Bank with the following accession codes: ChoX-choline (2REG), ChoX closed (2RF1), and ChoX-acetylcholine (2RIN).

RESULTS AND DISCUSSION

Choline and ACh Serve as Sole Carbon Sources for S. meliloti Strain 2011—The *S. meliloti* strain 2011 grows in minimal medium (25) supplemented with 0.2% (w/v) mannitol as the sole carbon source. Both choline and ACh can also serve as carbon sources for this microorganism, although growth was considerably reduced in comparison with the mannitol-supplemented culture (Fig. 1). It is thus apparent that *S. meliloti* can utilize both trimethylammonium compounds for nutritional

purposes although with reduced efficiency. The data reported by Dupont *et al.* (8) already suggested that the ChoVWX ABC transporter is capable of catalyzing the uptake of both choline and ACh.

Binding Activity of the Purified ChoX Protein—To obtain the *S. meliloti* ChoX protein for biochemical and structural analysis, we expressed the *choX* gene in *E. coli* from plasmid pETNx and overproduced ChoX as an N-terminal His-tagged fusion protein. ChoX was then purified by affinity chromatography to apparent homogeneity essentially as described by Dupont *et al.* (8). To assess the functionality of the purified ChoX protein, we performed a fluorescence-based equilibrium binding assay by exploiting the quenching of the intrinsic tryptophan fluorescence of ChoX upon substrate binding. From this type of experiment, the K_D value for choline was calculated to be 2.3 ± 1.0 μM (Fig. 2*A*). These data are in excellent agreement with the K_D value of 2.7 μM reported previously by Dupont *et al.* (8) that was based on a binding assay with radiolabeled choline. Using the fluorescence-based equilibrium binding assays, we also determined the K_D for ACh; a value of 100 ± 12 μM was derived (Fig. 2*B*). This K_D agrees reasonably well with that reported by Dupont *et al.* (8) (K_D = 145 μM) based upon binding studies with radiolabeled ACh and competition experiments. Hence the data reported by Dupont *et al.* (8) and the results reported here clearly establish ChoX as a binding protein for both choline (high affinity ligand) and ACh (medium affinity ligand), respectively.

Crystallization of ChoX and the Overall Fold of the Ligand-bound Protein—Crystals of the ChoX-choline complex were obtained by the hanging drop method at 277 K as described under "Experimental Procedures." The crystal structure was solved at 2.9-Å resolution by multiple wavelength anomalous dispersion phasing of an Se-Met derivative crystal. The structure of native ChoX in complex with choline was subsequently solved by molecular replacement at a resolution of 1.9 Å. Data statistics, refinement details, and model content are summarized in Table 1. The asymmetric unit contained two protomers. Because the r.m.s.d. of the two protomers is smaller than 0.5 Å for 288 Cα atoms, we will restrict the description of the overall ChoX structure and the architecture of the ligand-binding site to only one protomer. The overall structure of ChoX with bound choline (Fig. 3) shows a protein fold that is typical for bacterial SBPs (9, 14, 15). ChoX is an elliptical protein with dimensions of ~60 × 40 × 25 Å. Two globular domains (Fig. 3, colored *orange* and *blue*) are connected via two strands (residues 115–119 and 231–234) (Fig. 3, colored *yellow*). This topological arrangement of the protein backbone (Fig. 3) classifies ChoX as a type II ligand-binding protein (15). Domain I in the ChoX-choline model comprises residues 28–114 and 235–318 (Fig. 3, colored in *blue*). Residues 120–230 build up domain II (Fig. 3, colored *orange*). Both domains exhibit a central antiparallel five-stranded β-sheet with flanking helices common for type II binding proteins.

A comparison of domain I and domain II of ChoX clearly shows that the latter is not only smaller in size but also exhibits differences in secondary structure (Fig. 3). In domain II, β-strands F, G, and I are shorter than the corresponding β-strands in domain I. Interestingly β-strands D (residues

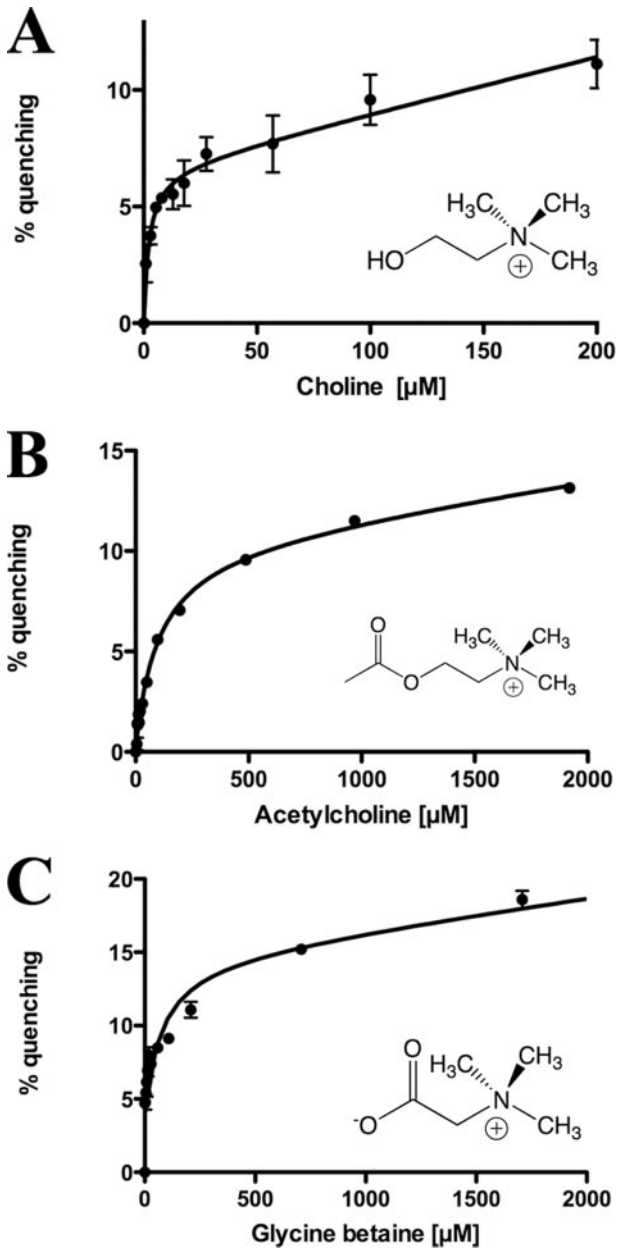

FIGURE 2. **Binding affinities of choline (*A*), acetylcholine (*B*), and glycine betaine (*C*) to ChoX were determined via intrinsic Trp quenching after the addition of the ligands to the ChoX protein.**

108–115) and E (residues 117–123) both extend into the linker between the two globular domains, basically forming one strand. This strand is disrupted by a single glycine residue (Gly^{116}), which itself is flanked by alanine residues. As glycine residues are known to contribute a rather high flexibility to the protein backbone (40), this amino acid and also the small adjacent alanine residues might play an important role in a movement of the two domains relative to each other upon substrate binding (14, 20).

One disulfide bridge (Cys^{33}-Cys^{247}) and two *cis*-peptide bonds (Met^{91}-Pro^{92} and Glu^{206}-Pro^{207}) are present in the ChoX-choline complex. The residues forming the disulfide bridge in ChoX both originate from domain I and covalently link helices 1 and 10. This disulfide bridge likely provides addi-

TABLE 1

Crystal parameters and data collection statistics

Crystal parameters and data collection statistics are derived from SCALEPACK (28) or XDS (29). Refinement statistics were obtained from REFMAC5 (31) or SHELXL (34). Data in parentheses correspond to the highest resolution shells. To calculate R_{free}, 5% of the reflections were excluded from the refinement. R_{sym} is defined as $R_{sym} = \Sigma_{hkl} \Sigma_i |I_i(hkl) - \langle I(hkl)\rangle| / \Sigma_{hkl} \Sigma_i I_i(hkl)$. R.m.s., root mean square; E.S.D., estimate standard deviation.

	Choline (native)	Choline (Se-Met)			Acetylcholine	Unliganded closed
Data collection						
Space group	$P2_1$		$P2_1$		$P2_1$	$P2_1$
Cell dimensions						
a, b, c [Å]	30.8, 185.4, 42.5	42.2, 210.3, 30.3			31.2, 212.7, 42.8	30.9, 196.2, 42.8
β [°]	91.8	91.3			90.1	90.1
		Peak	Inflection	Remote		
Wavelength	1.05	0.9791	0.9794	0.9500	0.98	1.033
Resolution [Å]*	93-1.9 (1.93-1.90)	105.4-2.9	105.4-2.9	105.4-2.9	20-1.8 (1.9-1.8)	20-2.0 (2.1-2.0)
R_{sym}*	4.5 (31.3)	9.0 (22.4)	7.2 (25.1)	7.1 (23.8)	4.0 (17.7)	6.6 (10.9)
I / σI*	16.7 (3.9)	20.4 (5.9)	13.5 (3.6)	13.1 (3.5)	14.9 (4.4)	14.6 (9.7)
Completeness [%]*	90.3 (83.7)	99.9 (98.7)	99.5 (97.6)	99.2 (95.5)	93.9 (87.6)	98.6 (99.1)
Redundancy	14.1	6.7	6.6	5.9	1.9	3.1
Unique reflections	37385	11694	11743	11693	48201	33779
Refinement						
Resolution [Å]	20-1.9				20-1.8	20-2.0
R_{work} / R_{free} [%]	18.0/22.2				15.1/21.0	20.1/23.6
Model content						
Protein	29- 318				29- 318	29- 318
Ligand	2				2	-
Water	269				236	197
Average B-factor [Å^2]	16.2				8.2	24.0
R.m.s deviations						
Bond lengths [Å]	0.007					
Bond angles [°]	1.052					
E. S. D.						
Bond lengths [Å]					0.007	0.001
Bond angles [Å]					0.027	0.013
Ramachandran plot [A]						
Favored [%]	97.7				92.3	94.8
Allowed [%]	2.3				7.4	4.9
Outliers [%]	–				0.3	0.3
Twinning fraction [B]	< 0.1				0.4775	0.495

* Values in parentheses correspond to the highest resolution shell.
[A] Derived from Molprobity.
[B] Derived from twin refinement in SHELXL.

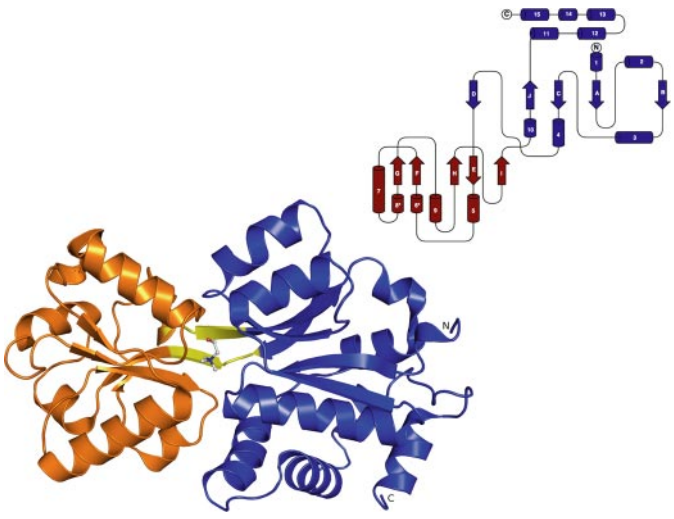

FIGURE 3. **Overall structure of the ChoX-choline complex.** Domains I and II are depicted in *blue* and *orange*, respectively. The linker connecting the domains is shown in *yellow*. Choline is shown in *ball-and-stick* representation. The *inset* shows the topology of ChoX. α-Helices are indicated by *numbers*, 3_{10}-helices are indicated by *numbers* and an *asterisk*, and β-strands are indicated by *letters*.

tional stability to the overall fold of ChoX. Disulfide bridges have, for instance, also been found in the crystal structures of the compatible solute-binding protein EhuB from *S. meliloti* that uses ectoine and hydroxyectoine as its substrates (39) and in the glycine betaine/proline betaine-binding protein ProX from *E. coli* (22). The two *cis*-peptide bonds present in the ChoX structure are of functional importance for the construction of the ligand-binding site. The structural consequences of these *cis*-peptide bonds on the proper positioning of the ligand-interacting side chains of Trp^{90} and Trp^{205} will be discussed in more detail below.

A DALI search revealed a number of substrate-binding proteins with high structural similarity to ChoX. Among the highest matches were the glycine betaine/proline betaine-binding protein ProX from *E. coli* (Z = 25.6 with 267 of the 309 Cα atoms aligning with an r.m.s.d. of 2.5 Å; Protein Data Bank code 1R9L) and the glycine betaine/proline betaine-binding protein ProX from the hyperthermophile *A. fulgidus* (Z = 22.2 with 241 of the 270 Cα atoms aligning with an r.m.s.d. of 2.5 Å; Protein Data Bank code 1SW4). The structural relatedness of these two compatible solute-binding proteins to ChoX suggests some similar principles of ligand binding despite the rather medium overall amino acid sequence identity of the two ProX proteins to ChoX (19 and 17%, respectively).

The Choline-binding Site within the ChoX Protein—The ligand choline binds in a deep gorge between the two globular domains of ChoX (Fig. 3). A closer inspection of the binding site indicates that residues from domain I as well as domain II (Fig. 4) build up an aromatic box consisting of three tryptophans and a single tyrosine residue (Trp^{43} (N-terminally of helix 2, domain I), Trp^{90} (β-sheet C, domain I), and Trp^{205} (β-sheet H, domain II) and Tyr^{119} (β-sheet E, at the N terminus of domain II)). Together these four aromatic side chains coordinate the positioning of the trimethylammonium head moiety of choline in the ligand binding pocket (Fig. 4). Within the head group of choline, the positive charge is not fixed on the nitrogen atom of the choline molecule but instead is delocalized over the three methyl groups thereby resulting in the formation of a bulky cation (22). The binding of this voluminous cation within the aromatic ligand-binding box of ChoX is established via cation-π interactions (41, 42). Distances between the carbon atom in the methyl groups of the choline head group and the aromatic side chains of Trp^{43}, Trp^{90}, Trp^{205}, and Tyr^{119} are in the range of ~3.5–4 Å, consistent with the van der Waals radii of these atoms (43). In the case of bound choline, 28 interactions are observed. Additionally the choline head group forms a salt bridge with Asp^{45} (distances of 3.3 and 3.8 Å) that originates from domain I (Fig. 4).

Interestingly the two *cis*-peptide bonds present in ChoX (Met^{91}-Pro^{92} and Glu^{206}-Pro^{207}) are positioned C-terminally to Trp^{90} and Trp^{205}, which both are part of the ligand-binding site (Fig. 4). This strongly suggests that a *cis*-conformation of the protein backbone is necessary at these positions to create the required geometry of the ligand-binding site. Indeed a *trans*-conformation of these two peptide bonds would position Pro^{92} and Pro^{205} in very close distance to the bound ligand. The "tail" of the choline molecule, consisting of a hydroxyl group, forms hydrogen bonds with Asn^{156} and Asp^{157} (distances of 2.7 and 3.0 Å, respectively) (Fig. 4). In summary, the choline head group interacts via cation-π interactions with residues contributed by both domains I and II of ChoX, whereas the tail of choline is bound exclusively by residues originating from domain II (Fig. 4). In addition, two water molecules (shown in Fig. 4 as *blue spheres*) bridge the side chain of Asp^{45} with the indole moieties of Trp^{43} (domain I) and Trp^{205} (domain II). These additional

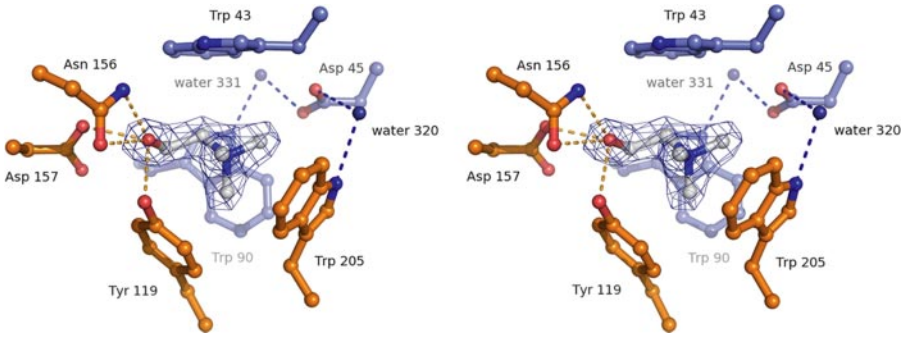

FIGURE 4. **Stereoview of the choline-binding site.** Choline is shown in *ball-and-stick* representation. Residues of domains I and II forming the ligand-binding site are colored in *blue* and *orange*, respectively. An electron density of the substrate is presented as a 1 $F_o - F_c$ omit map countered at 3σ after omission of choline from the refinement. *Dashed lines* highlight interactions between the ligand and amino acid residues. For simplicity, cation-π interactions of the trimethylammonium head group of choline and the aromatic amino acids forming the aromatic box are not shown.

interactions apparently further stabilize the ligand-binding site in the ligand-bound closed state of ChoX.

An architecture of ligand-binding sites similar to that revealed in ChoX has been found previously in compatible solute-binding proteins for glycine betaine and proline betaine, ProX from *E. coli*, OpuAC from *B. subtilis*, and ProX from *A. fulgidus* (21–24). The trimethylammonium head group of glycine betaine and the dimethylammonium head group of proline betaine exhibit delocalized positive charges similar to those of choline. Consequently cation-π interactions of these ligands with aromatic residues lining the substrate-binding sites are commonly used by the ChoX, ProX, and OpuAC proteins to ensure high affinity substrate binding. Mutational analysis has been used to probe the importance of individual aromatic residues within the binding pockets of ProX from *E. coli* (22), OpuAC from *B. subtilis* (24), and the ectoine/hydroxyectoine-binding protein EhuB from *S. meliloti* that also uses cation-π interactions for compatible solute binding (39). In each case, the strength of the cation-π interactions are key determinants for efficient ligand binding, but the contributions of individual aromatic residues to substrate binding are different in ProX, OpuAC, and EhuB as is the precise geometry of the aromatic ligand-binding box (21–24, 39).

As observed here for the ChoX-choline complex, salt bridges or hydrogen bonds between the negatively charged carboxylates of glycine betaine, proline betaine, and ectoine/hydroxyectoine are used to further stabilize the substrate within the binding pockets of their respective binding proteins (21–24, 39). It is also worth noting that as in ChoX two *cis*-peptide bonds within the *E. coli* ProX polypeptide chain (22) provide for a bend in the protein backbone. These structural characteristics are required to properly position aromatic residues in the binding pocket for effective interactions with the ligand.

The Acetylcholine-binding Site of the ChoX Protein—Attempts to co-crystallize ChoX and ACh resulted in diffracting crystals. However, structure determination revealed that the substrate ACh was hydrolyzed during the time required for crystal formation (4 weeks) and that only choline was present in the ligand-binding site. Therefore, we used streak seeding (see "Experimental Procedures" for details) to rapidly obtain crystals of the ChoX-ACh complex (27). This approach was successful, and well diffracting crystals of the ChoX-ACh complex could be generated. The asymmetric unit contained two protomers, and the structure of the ChoX-ACh complex was refined to 1.8-Å resolution. A summary of the crystallographic data and refinement statistics is given in Table 1. Because the overall fold of ChoX with either choline or ACh as ligand is identical (r.m.s.d. $<$0.5 Å for 288 Cα atoms), we will restrict the description of the structure of the ChoX-ACh complex to the ligand-binding site.

The architecture of the binding sites within the ChoX-ACh complex and the geometry of the substrate ACh within the binding site differ slightly in the two protomers of the asymmetric unit (Fig. 5, *A* and *B*). The trimethylammonium head group of ACh is similarly bound in the two protomers via cation-π interactions to an aromatic box composed of Trp^{43}, Trp^{90}, Tyr^{119}, and Trp^{205}. Hence the same type of molecular interactions and the same interaction partners are used to coordinate the binding of the positively charged head groups of either choline (Fig. 4) or ACh (Fig. 5, *A* and *B*) within ChoX. Overall the cation-π interactions within this aromatic box generate 23 contacts. Furthermore a few short distances in the range of 3–3.3 Å between ACh and the aromatic residues are observed that could possibly impose repulsive interactions (four and three in monomers A and B, respectively). Furthermore the trimethylammonium head group of ACh is fixed via a salt bridge to the side chain of Asp^{45} (Fig. 5, *A* and *B*). The binding of the bulky cation head group of ACh to Asp^{45}, as measured from the carbon of the nearest methyl group of ACh to the oxygen of Asp^{45}, is tighter in monomer A (Fig. 5*A*; 2.8 Å) than in monomer B (Fig. 5*B*; 3.2/3.6 Å); this is because of slightly different positions of the trimethylammonium head group of ACh and the carbonyl group of Asp^{45}. Additionally Asp^{45} interacts with Trp^{90} and Trp^{205} through two water molecules, thereby further stabilizing the liganded-closed state of ChoX (Fig. 5, *A* and *B*).

The major difference between the two ACh molecules of the two ChoX protomers lies within the binding geometry of the acetyl group. Whereas the trimethylammonium groups of both molecules occupy similar positions, the tail of the substrates point to different directions. The torsion angles between carbonyl carbon of the acetyl group and the methylene carbon of the choline group thus show values of 92° and 55° for ACh in monomers A and B, respectively. Therefore, in monomer B the ACh adopts a slightly more compact conformation. In both monomers (Fig. 5, *A* and *B*) hydrogen bonds are formed by the carbonyl oxygen of acetylcholine, one with the amide group of Asn^{156} and a second one with Asp^{157}, if this residue exhibits a protonated state. Both these residues are contributed by domain II of ChoX. It is possible that the different arrangements of the ligand-binding site reflect two different binding modes for the substrate ACh. However, an analysis of the mean B-factor for ACh shows an elevated value of 17.4 $Å^2$ for mono-

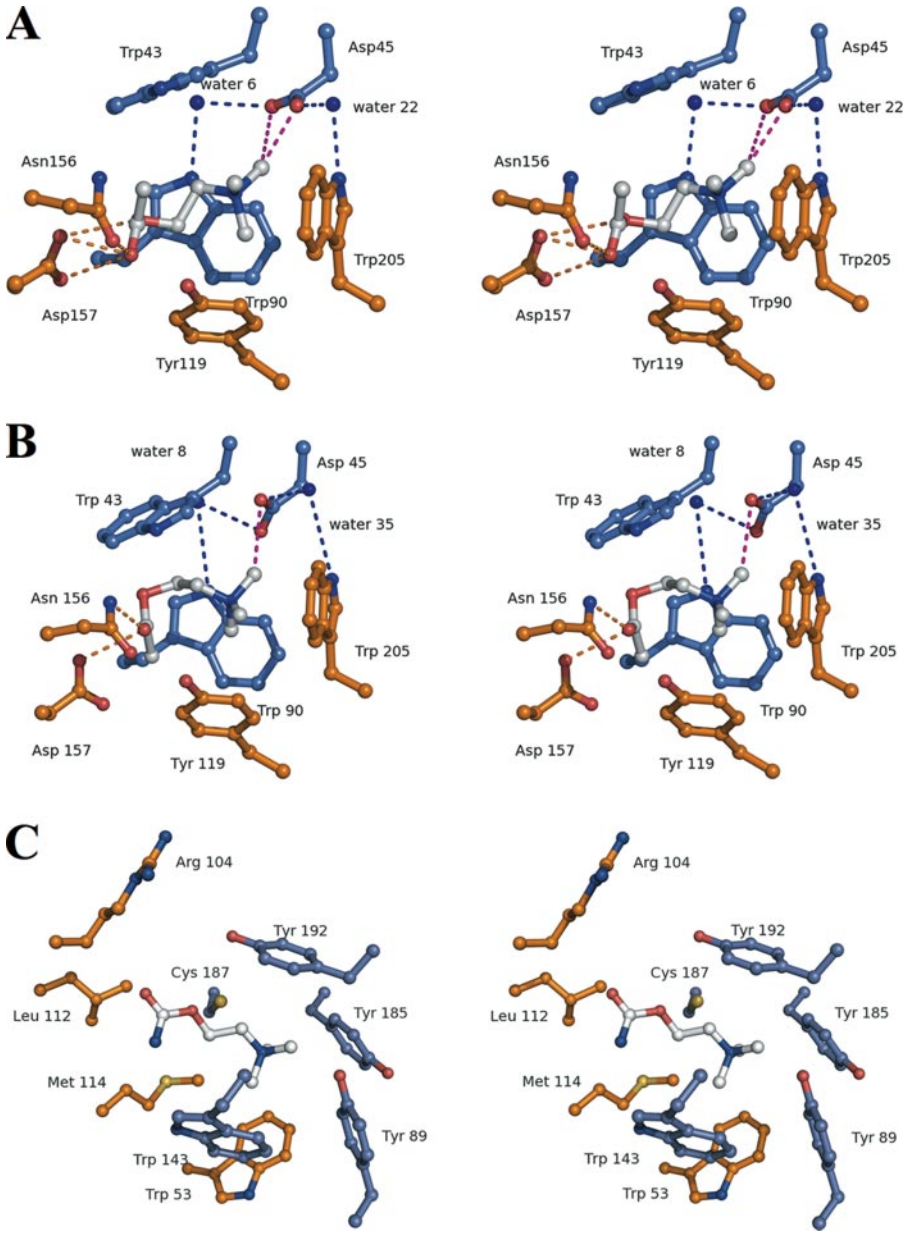

FIGURE 5. Stereorepresentation of the acetylcholine-binding site in monomer A (*A*) and monomer B (*B*) of the asymmetric unit is shown. Residues located in domain I are highlighted in *blue*; residues originating from domain II are shown in *orange*. The two water molecules that connect Asp[45] (domain I) with Trp[90] or Trp[205] (domain II) are shown as *blue spheres*. *C*, stereoview of the binding site of the AChBP-carbamylcholine complex (Protein Data Bank code 1UV6) from *L. stagnalis* (45). Carbamylcholine is shown in *ball-and-stick* representation. Residues of the principal side of AChBP are colored in *blue*; residues from the complementary side of AChBP are colored in *orange*.

mer B in comparison with monomer A (8.5 Å^2). Also the electron density of the ACh in monomer A is better defined than in monomer B. Therefore, it cannot be ruled out that the observed different binding geometries of the ligand in the two monomers are simply because of higher thermal motion of ACh in monomer A.

Comparision of ACh Binding in ChoX from S. meliloti Versus Carbamylcholine Binding in Acetylcholine-binding Protein (AChBP) from Lymnaea stagnalis—The AChBP from the mollusc *L. stagnalis* is widely considered as a water-soluble homologue of the ligand-binding domain of the membrane-bound nicotinic acetylcholine receptor proteins that are of great pharmacological importance (44). The crystal structure of AChBP has been solved previously by Celie *et al.* in complex with carbamylcholine (Protein Data Bank code 1UV6), a non-hydrolyzable analogue of ACh (45). The AChBP and ChoX proteins are not related to each other in their overall folds; furthermore the biologically active species of AChBP is a pentamer, whereas ChoX is a monomer. However, a comparison of the architecture of the ligand binding pockets of these two proteins revealed common structural elements and mode of substrate recognition by acetylcholine-binding proteins of either eukaryotic or prokaryotic origin.

First in both structures the trimethylammonium moieties of either carbamylcholine or ACh contact aromatic residues via cation-π interactions. In the AChBP structure (Fig. 5*C*), five aromatic residues build up an aromatic box similar to the one found in ChoX (Fig. 5, *A* and *B*). The aromatic box of AChBP consists of two tryptophans and three tyrosines, whereas in ChoX, three tryptophans and one tyrosine residue form the aromatic box.

In the binding site of AChBP from *L. stagnalis*, the substrate carbamylcholine is bound between two separate subunits of the pentameric complex (45). Residues from two subunits, called the principal and the complementary sides (45), contribute to the formation of the binding site (Fig. 5*C*). The binding of ACh to ChoX involves only one protein, but as outlined above, residues from both domains of ChoX contribute to ligand binding (Fig. 5, *A* and *B*). Because residues originating from both domain I and domain II of ChoX (Fig. 3) form the binding site, the principal and complementary sides present in AChBP (Fig. 5*C*) is reflected in the binding of the trimethylammonium head groups of either carbamylcholine or ACh. In contrast, the binding of the tail of the ligands is accomplished by only one domain of AChBP or ChoX. These are the complementary side in AChBP and domain II in ChoX. Whereas the tail of carbamylcholine in AChBP makes weak contacts with the hydrophobic amino acids Leu[112] and Met[114] (Fig. 5*C*), the tail of the ACh in the ChoX-ACh complex makes contacts with Asp[157] and Asn[156]; both are highly polar amino acids contributed by domain II of ChoX (Fig. 5, *A* and *B*). In addition, further

stabilizing hydrogen bonds are established between the tail of ACh to Tyr^{119}, a residue that also originates from domain II of ChoX (Fig. 5, *A* and *B*).

The Unliganded-Closed Conformation of the ChoX Protein—We attempted to crystallize the ChoX protein in the absence of a ligand via seeding (27) to gain structural insights into the open, unliganded form of this binding protein. These attempts were not successful. Instead we obtained crystals that upon structural analysis revealed a closed but unliganded form of the ChoX protein. Although many structures are known of substrate-binding proteins in either their unliganded-open or liganded-closed states (9, 14, 15), up to now only one crystal structure has been published for a microbial substrate-binding protein in its unliganded-closed state. This is the crystal structure of the galactose/glucose-binding protein (GGBP) from *Salmonella typhimurium* reported by Flocco and Mowbray (19) in 1994.

The structure of ChoX in its unliganded-closed conformation was refined to a resolution of 2.0 Å and is therefore directly comparable with the structure of ChoX in complex with choline at a resolution of 1.9 Å (Table 1). Data statistics for the ChoX unliganded-closed conformation, refinement details, and model content are summarized in Table 1. The three-dimensional structures of GGBP and ChoX in the closed, unliganded forms suggest that substrate-binding protein can adopt a closed conformation in the absence of a ligand. The closed but unliganded forms of GGBP and ChoX provide further credence to the proposal that substrate-binding proteins constantly undergo closing and opening movements around their hinge regions even in the absence of a ligand (9, 14–16, 19, 20). Comparing the overall structures of the liganded-closed and unliganded-closed states of ChoX did not reveal any significant differences (r.m.s.d. <0.2 Å for 288 Cα atoms) (Fig. 6*A*). The overall fold of the two ChoX structures is virtually identical despite the fact that they represent functionally completely different states of the ChoX protein with respect to the overall transport process. Likewise the closed, unliganded and closed, ligand-bound forms of GGBP also exhibited very similar overall folds, but the former protein was crystallized in a form that was slightly more "open" than the liganded form (19).

Of particular interest is the comparison of the substrate binding pocket of ChoX in its closed, ligand-bound form with its closed, unliganded form (Fig. 6, *B* and *C*). All amino acids participating in ligand binding are in place in the unliganded-closed ChoX protein thereby preserving the general architecture of the substrate-binding site as observed in the liganded form of ChoX (Fig. 6*B*). A superimposition of the binding pockets from the closed, ligand-bound and closed, unliganded forms of ChoX (Fig. 6*C*) revealed an r.m.s.d. for the Cα atoms of the residues forming the binding site of 0.2 Å. The only differences between the two structures are the absence of the ligand and the presence of three water molecules instead of choline within the ligand-binding site in the unliganded-closed state. The presence of water molecules is reminiscent of the crystal structure of GGBP in its unliganded-closed form (19) and suggests that these water molecules in both GGBP and ChoX substitute for the ligand.

Ames *et al.* (46) observed identical affinities for the liganded and ligand-free substrate-binding protein HisJ from the histidine transporter of *S. typhimurium*. The absence of any structural difference between the liganded-closed and unliganded-closed states of either ChoX (this study) or GGBP (19) raises the question of why a substrate-loaded SBP is capable to more strongly stimulate ATPase activity of the transporter in an *in vitro* assay than the substrate-free form of the binding protein (47, 48). From a structural point of view, the reported biochemical data cannot be adequately explained, and this issue clearly requires further investigations. Understanding how ABC transporters are capable of distinguishing the liganded-closed and unliganded-closed states of their cognate binding proteins is even more important in light of theoretical, biochemical, and structural investigations (46–51). For example, it was interfered from small angle x-ray crystallography that the maltose-binding protein could exist as a mixture of 85% open and 15% closed forms in the absence of ligand (51). However, recent NMR studies (52) have demonstrated that the liganded-closed state of maltose-binding protein is different from the one observed by x-ray crystallography for GGBP and ChoX. Based on the detected NMR restraints, the authors concluded that the unliganded-closed state, which is present at an amount of 5% in the absence of ligand, is not simply the mirror image of the liganded-closed state but rather a twisted form (52). This is likely because of the negatively charged ligand-binding site of maltose-binding protein that predicts an energy difference of 16 kcal/mol for the liganded state and a "GGBP-like" unliganded-closed state (53). However, as already pointed out by Millet et *al.* (53), the situation is different for GGBP. Here hydrogen bonds and water molecules from both domains provide the stabilization in the absence of ligand. This is fundamentally different from maltose-binding protein. In the case of ChoX, the architecture of the ligand-binding site (hydrogen bonds, cation-π interactions, and water molecules) is similar to GGBP and different from maltose-binding protein. Thus, it is likely that the architecture of ChoX and its ligand-binding site creates an environment that is reminiscent of GGBP with respect to the closed state.

ChoX as a Functional and Structural Template for Other Microbial Substrate-binding Proteins—A BLAST search for protein related to the amino acid sequence of the *S. meliloti* ChoX protein was conducted using the NCBI network service. ChoX-related proteins were readily detected, and the top 75 ChoX-related proteins were retained for further analysis (data not shown). Each of these proteins is annotated in the NCBI data base as a putative substrate-binding protein of microbial ABC transport systems. Most of these ChoX-related proteins are from Gram-negative bacteria, they have about the same number of amino acids as ChoX, and the amino acid sequences of these proteins readily align without major gaps with the ChoX sequence resulting in an amino acid sequence identity ranging from 96 to 49%. The proteins that are most closely related to ChoX from *S. meliloti* are proteins from *Sinorhizobium medicae* strain WSM419 (96% sequence identity), *Agrobacterium tumefaciens* strain C58 (79% sequence identity), *Rhizobium etli* strain CFN42 (74% sequence identity), and *Rhizobium leguminosarum* bv. Vivicae strain 38412 (74% sequence

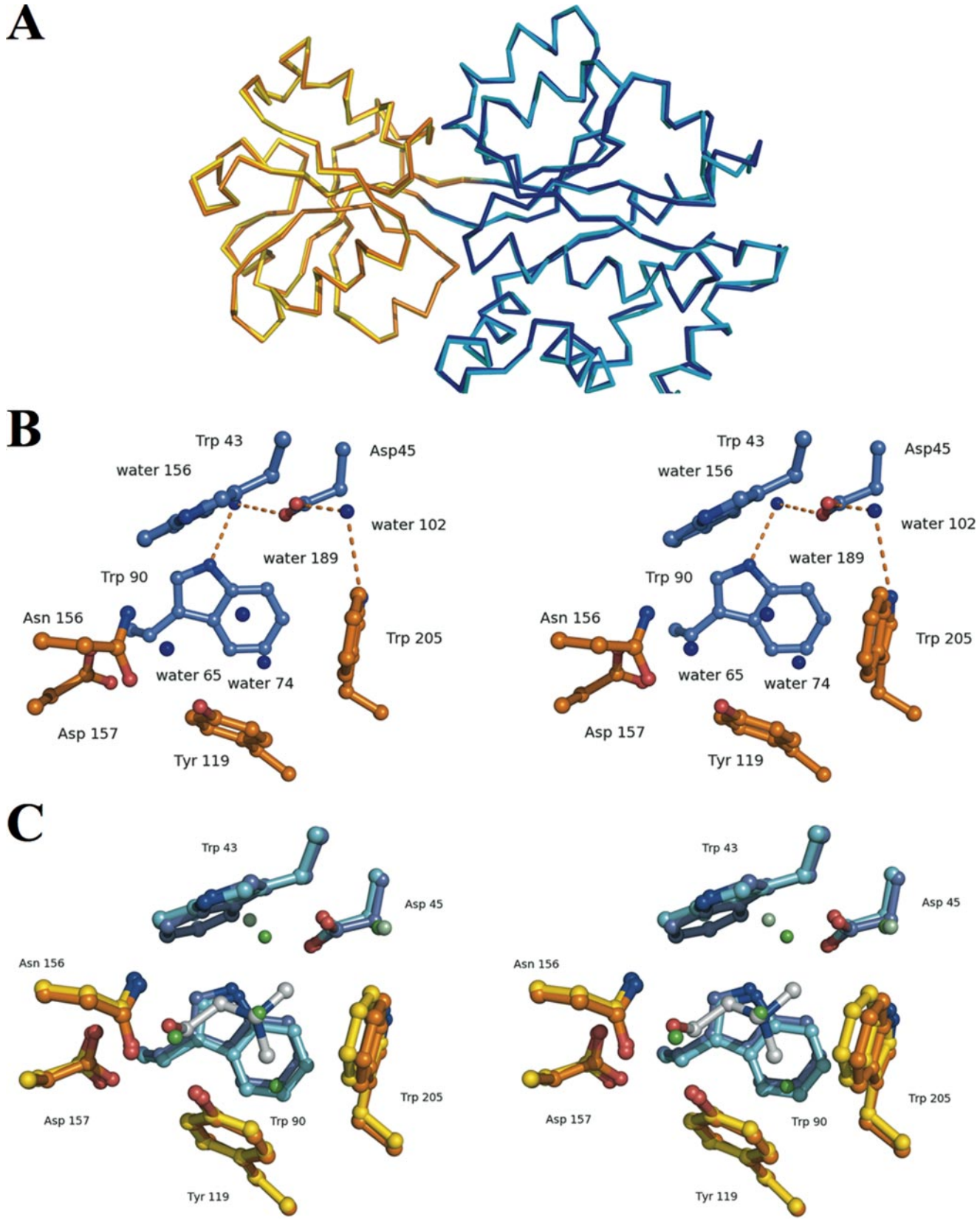

FIGURE 6. *A*, overall structural superimposition of the liganded-closed and the unliganded-closed state of ChoX. The liganded-closed state is colored in *blue* (domain I) and *orange* (domain II), and the unliganded-closed state is colored in *cyan* (domain I) and *yellow* (domain II). For simplicity the ligand was omitted, and residues belonging to the linker region are not highlighted by a specific color. *B*, stereoview of the ligand-binding site of the unliganded-closed state of ChoX. Residues of domain I are shown in *blue*, and residues of domain II are shown in *orange*. Water molecules are shown as *blue spheres* and *numbered* according to their Protein Data Bank files. *C*, stereoview of a structural superposition of the ligand-binding sites of closed-liganded and closed-unliganded ChoX structures. Residues originating from domain I are depicted in *blue* (liganded) and *cyan* (unliganded), and residues from domain II are depicted in *orange* (liganded) and *yellow* (unliganded). Choline is shown in *ball-and-stick* representation, and water molecules are shown as *light green* (liganded) and *green spheres* (unliganded).

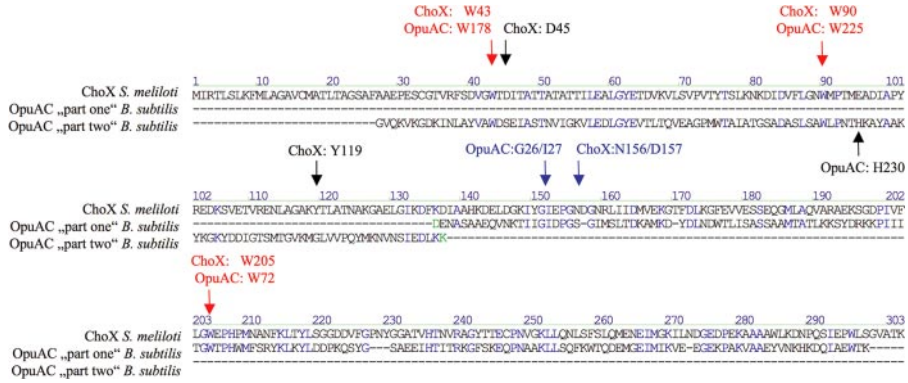

FIGURE 7. **Sequence alignment of the OpuAC and ChoX proteins.** The amino acid sequence of the glycine betaine/proline betaine-binding protein OpuAC from *B. subtilis* is aligned with the amino acid sequence of the choline/acetylcholine-binding protein ChoX protein from *S. meliloti*. To align both sequences, an in-domain cut was taken into account by splitting the OpuAC sequence between amino acids 168 and 169 (highlighted in *green*) and then using the inverted N- and C-terminal portions of OpuAC for the sequence alignment as detailed by Horn *et al.* (21) and Smits *et al.* (24). Residues involved in ligand binding in either ChoX or OpuAC are marked.

identity). Each of these microorganisms is taxonomically closely related to *S. meliloti*.

We inspected the alignment of the 75 ChoX-related substrate-binding proteins for the conservation of those residues that are involved in either choline or acetylcholine binding by ChoX. The three Trp residues (Trp^{43}, Trp^{90}, and Trp^{205}) that interact with the cation head group of either choline (Fig. 4) or acetylcholine (Fig. 5, *A* and *B*) are completely conserved. Likewise Tyr^{119} that is also involved in ligand binding via cation-π interactions with the head group of the ChoX ligands (Figs. 4 and 5, *A* and *B*) is also highly conserved and is only replaced in a few proteins (more distantly related to ChoX) by either Phe or Ala residues. Furthermore Asp^{45} that also makes contacts to the choline or acetylcholine head groups (Figs. 4 and 5, *A* and *B*) via a salt bridge is completely conserved within the compiled group of 75 ChoX-related proteins. Asn^{156} and Asp^{157} make stabilizing contacts to the tail of both choline (Fig. 4) and acetylcholine (Fig. 5, *A* and *B*) via hydrogen bonds; both residues are highly conserved and are only replaced by other residues in proteins more distantly related to ChoX that also can form hydrogen bonds. We also note that the two Pro residues (Pro^{92} and Pro^{207}) that induce the formation of the two *cis*-peptide bonds in ChoX that are required for the proper positioning of the ligand-interacting Trp^{90} and Trp^{205} residues are fully conserved. Likewise the residues corresponding to Cys^{33} and Cys^{247} forming the sole disulfide bridge in ChoX are fully conserved in the 75 aligned ChoX-related proteins, indicating that this disulfide bridge is an important structural element for ChoX-type proteins. Consequently the framework of those residues contributing to the architecture of the choline and acetylcholine ligand-binding site within ChoX are all in place within an evolutionarily related group of substrate-binding proteins.

It is worth noting that none of the ChoX-related proteins compiled by us is currently annotated in the NCBI data base as either a choline- or acetylcholine-binding protein. Instead these proteins are either neutrally annotated as SBPs of ABC-type transporters or specifically annotated as putative glycine betaine/proline betaine substrate-binding proteins. Our analysis of this group of proteins, guided by the structure of ChoX and its interactions with its two ligands, predicts that most, if not all, of the 75 ChoX-related proteins should be able to actually bind choline and acetylcholine as their substrates. Furthermore we consider it likely that each of these proteins will adopt a fold similar to the structure of ChoX reported here.

Alignment of the Choline/Acetylcholine-binding Protein ChoX with the Glycine Betaine-binding Protein OpuAC Predicts That ChoX Should Also Bind Glycine Betaine—OpuAC is an extracellular lipoprotein that serves as the substrate-binding protein for the compatible solute ABC transporter OpuA from *B. subtilis* (54). The crystal structure of OpuAC in complex with its high affinity ligand glycine betaine (K_D = 17 μM) has recently been solved by Horn *et al.* (21). The trimethylammonium head group of glycine betaine is coordinated within the OpuAC binding site via cation-π interactions with three Trp residues (Trp^{72}, Trp^{178}, and Trp^{225}) arranged in the form of a prism. Further stabilizing contacts between the substrate and OpuAC are made via hydrogen bonds between the carboxylate of glycine betaine and His^{230} and to the backbone amides of Gly^{26} and Ile^{27} (21). Mutational analysis of the residues forming the ligand-binding site in OpuAC has shown that each of the three Trp residues is essential for efficient glycine betaine binding and that the formation of the hydrogen bond between the ligand and His^{230} is a key element for the high affinity binding of this ligand by OpuAC (24).

Many OpuAC-related proteins are present in the NCBI data base, but in most cases an efficient alignment of these proteins to OpuAC can only been made when an "in-domain cut" (21) in the OpuAC sequence between residues 168 and 169 is applied and the N- and C-terminal segments are then inverted in the sequence alignments (21, 24). We found that the *S. meliloti* ChoX and *B. subtilis* OpuAC proteins can be aligned when the in-domain cut is applied to OpuAC (Fig. 7). The three Trp residues that coordinate the binding of the positively charged head group of glycine betaine via cation-π interactions in OpuAC and the Gly^{26}-Ile^{27} residues that serve as interacting partners for the carboxylic tail of glycine betaine are also present in ChoX, whereas the functionally important His^{230} residue found in OpuAC is missing in ChoX (Fig. 7). In contrast, Tyr^{119} and residues Asn^{156}-Asp^{157} that participate in the binding of both choline and acetylcholine in ChoX have no functionally equivalent counterparts in OpuAC (Fig. 7).

The structure-guided inspections of the OpuAC and ChoX sequences suggested that ChoX should actually be able to bind glycine betaine albeit with modest efficiency because the important His^{230} equivalent residue from OpuAC is missing in ChoX. However, in connection with the initial analysis of the substrate specificity of ChoX via competition experiments, Dupont *et al.* (8) reported that ChoX does not bind glycine betaine. In light of the above observations, we re-examined the

binding properties of ChoX, and utilizing the fluorescence-based equilibrium binding assay (see Fig. 2) we found that ChoX can actually bind glycine betaine with an affinity (K_D of 77 ± 21 μM) (Fig. 2*C*) that lies between those of its ligands choline (K_D of 2.3 ± 1.0 μM) and acetylcholine (K_D of 100 ± 21 μM) (Fig. 2). Compared with OpuAC, this reduced affinity is likely because of the fact that the His residue of OpuAC that is important for the high affinity binding of glycine betaine is exchanged to a Glu residue in ChoX. If the glutamate is not protonated, the repulsion between its negatively charged side chain and carboxylate moiety of glycine betaine would result in weaker binding explaining the differences in K_D. Hence a prediction for a new substrate of ChoX could be made, and experimentally verified, by comparing the functionally important residues form the ligand binding pockets of ChoX and OpuAC.

Conclusions—Here we presented the crystal structures of two substrate-bound species of ChoX, a periplasmic ligand-binding protein from the plant root-associated soil bacterium *S. meliloti*. The overall fold of ChoX closely resembles that of many substrate-binding proteins of microbial ABC-type transport systems. However, the structures of the ChoX-choline and ChoX-acetylcholine complexes reported here uncovered for the first time the molecular details of choline and acetylcholine recognition by a microbial substrate-binding protein. Data base searches revealed a substantial number of ChoX-related binding proteins in a wide range of microbial species, and our ChoX structure-guided inspection of these proteins suggests that they might all function in choline and acetylcholine binding. After a structure-guided comparison of the residues involved in ligand binding in the OpuAC and ChoX proteins, we were able to predict that ChoX should actually also bind glycine betaine and verified this prediction experimentally. The mode of ligand binding found in ChoX for acetylcholine can also be found in the AChBP from the mollusc *L. stagnalis* (45) that is a water-soluble homologue of the ligand-binding domain of membrane-bound acetylcholine receptors (44) but that is totally unrelated in amino acid sequence and biological function to ChoX. We were also able to obtain crystals of ChoX in a substrate-free closed conformation. This form of ChoX revealed an architecture of the ligand-binding site that is perfectly superimposable to the closed, ligand-bound form of ChoX. Only one structure of a single, closed, and unliganded form of another binding protein, GGBP from *S. typhimurium*, has been reported previously (19). The closed, unliganded structures of ChoX and GGBP support the view that certain binding proteins can fully close in the absence of a ligand.

Acknowledgments—We thank Nils Hanekop, Robert Ernst, and Justin Lecher for many helpful and stimulating discussions. We are indebted to Gleb Bourenkov and Mathew Groves for constant and excellent support during data acquisition at the Max-Planck-Gesellschaft and European Molecular Biology Laboratory beam lines at Deutsches Elektronen Synchrotron, Hamburg, Germany and advice during the refinement process. We also thank Eckhard Hoffmann, Gleb Bourenkov, and George Sheldrick for advice during the refinement of the twinned crystals. M. H. and E. B. thank Maritha Lippmann for expert technical support.

REFERENCES

1. Kortstee, G. J. (1970) *Arch. Microbiol.* **71,** 235–244
2. Long, S. R. (1989) *Cell* **56,** 203–214
3. Bernard, T., Pocard, J. A., Perroud, B., and Lerudulier, D. (1986) *Arch. Microbiol.* **143,** 359–364
4. Osteras, M., Boncompagni, E., Vincent, N., Poggi, M. C., and Le Rudulier, D. (1998) *Proc. Natl. Acad. Sci. U. S. A.* **95,** 11394–11399
5. de Rudder, K. E. E., Sohlenkamp, C., and Geiger, O. (1999) *J. Biol. Chem.* **274,** 20011–20016
6. Lopez-Lara, I. M., Sohlenkamp, C., and Geiger, O. (2003) *Mol. Plant-Microbe Interact.* **16,** 567–579
7. Pocard, J. A., Bernard, T., Smith, L. T., and Le Rudulier, D. (1989) *J. Bacteriol.* **171,** 531–537
8. Dupont, L., Garcia, I., Poggi, M. C., Alloing, G., Mandon, K., and Le Rudulier, D. (2004) *J. Bacteriol.* **186,** 5988–5996
9. Davidson, A. L., Dassa, E., Orelle, C., and Chen, J. (2008) *Microbiol. Mol. Biol. Rev.* **72,** 317–364
10. Biemans-Oldehinkel, E., Doeven, M. K., and Poolman, B. (2006) *FEBS Lett.* **580,** 1023–1035
11. Hollenstein, K., Frei, D. C., and Locher, K. P. (2007) *Nature* **446,** 213–216
12. Hvorup, R. N., Goetz, B. A., Niederer, M., Holenstein, K., Perozo, E., and Locher, K. P. (2007) *Science* **317,** 1387–1390
13. Oldham, M. L., Khare, D., Quiocho, F. A., Davidson, A. L., and Chen, J. (2007) *Nature* **450,** 515–521
14. Quiocho, F. A., and Ledvina, P. S. (1996) *Mol. Microbiol.* **20,** 17–25
15. Wilkinson, J., and Verschueren, K. H. G. (2003) in *ABC Proteins: from Bacteria to Man* (Holland, I. B., Cole, S. P. C., Kuchler, K., and Higgins, C. F., eds) pp. 178–208, Academic Press (Elsevier Science), London
16. Sack, J. S., Saper, M. A., and Quiocho, F. A. (1989) *J. Mol. Biol.* **206,** 171–191
17. Magnusson, U., Chaudhuri, B. N., Ko, J., Park, C., Jones, T. A., and Mowbray, S. L. (2002) *J. Biol. Chem.* **277,** 14077–14084
18. Bjorkman, A. J., and Mowbray, S. L. (1998) *J. Mol. Biol.* **279,** 651–664
19. Flocco, M. M., and Mowbray, S. L. (1994) *J. Biol. Chem.* **269,** 8931–8936
20. Mao, B., Pear, M. R., McCammon, J. A., and Quiocho, F. A. (1982) *J. Biol. Chem.* **257,** 1131–1133
21. Horn, C., Sohn-Bosser, L., Breed, J., Welte, W., Schmitt, L., and Bremer, E. (2006) *J. Mol. Biol.* **357,** 592–606
22. Schiefner, A., Breed, J., Bosser, L., Kneip, S., Gade, J., Holtmann, G., Diederichs, K., Welte, W., and Bremer, E. (2004) *J. Biol. Chem.* **279,** 5588–5596
23. Schiefner, A., Holtmann, G., Diederichs, K., Welte, W., and Bremer, E. (2004) *J. Biol. Chem.* **279,** 48270–48281
24. Smits, S. H., Hoing, M., Lecher, J., Jebbar, M., Schmitt, L., and Bremer, E. (2008) *J. Bacteriol.* **190,** 5663–5671
25. Miller, J. H. (1972) *Experiments in Molecular Genetics*, Cold Spring Harbor Laboratory Press, Cold Spring Harbor, NY
26. Abele, R., Keinanen, K., and Madden, D. R. (2000) *J. Biol. Chem.* **275,** 21355–21363
27. Oswald, C., Smits, S. H. J., Bremer, E., and Schmitt, L. (2008) *Int. J. Mol. Sci.* **9,** 1131–1141
28. Otwinowski, Z., and Minor, W. (1997) in *Methods in Enzymology* (Carter, C. W., and Sweet, R. M., eds) Vol. 276, pp. 307–325, Academic Press, London
29. Kabsch, W. (1993) *J. Appl. Crystallogr.* **26,** 795–800
30. Terwilliger, T. C., and Berendzen, J. (1999) *Acta Crystallogr. Sect. D Biol. Crystallogr.* **55,** 849–861
31. Murshudov, G., Vagin, A. A., and Dodson, E. J. (1997) *Acta Crystallogr. Sect. D Biol. Crystallogr.* **53,** 240–255
32. Emsley, P., and Cowtan, K. (2004) *Acta Crystallogr. Sect. D Biol. Crystallogr.* **60,** 2126–2132
33. Vagin, A., and Teplyakov, A. (2000) *Acta Crystallogr. Sect. D Biol. Crystallogr.* **56,** 1622–1624
34. Sheldrick, G. M., and Schneider, T. R. (1997) in *Methods in Enzymology* (Carter, C. W., and Sweet, R. M., eds) Vol. 277, pp. 319–343, Academic Press, London
35. Lamzin, V. S., and Wilson, K. S. (1993) *Acta Crystallogr. Sect. D Biol. Crystallogr.* **49,** 129–147

36. Davis, I. W., Leaver-Fay, A., Chen, V. B., Block, J. N., Kapral, G. J., Wang, X., Murray, L. W., Arendall, W. B., III, Snoeyink, J., Richardson, J. S., and Richardson, D. C. (2007) *Nucleic Acids Res.* **35,** W375–W383
37. Altschul, S. F., Madden, T. L., Schaffer, A. A., Zhang, J., Zhang, Z., Miller, W., and Lipman, D. J. (1997) *Nucleic Acids Res.* **25,** 3389–3402
38. Thompson, J. D., Higgins, D. G., and Gibson, T. J. (1994) *Nucleic Acids Res.* **22,** 4673–4680
39. Hanekop, N., Hoing, M., Sohn-Bosser, L., Jebbar, M., Schmitt, L., and Bremer, E. (2007) *J. Mol. Biol.* **374,** 1237–1250
40. Ramachandran, G. N., Ramakrishnan, C., and Sasisekharan, V. (1963) *J. Mol. Biol.* **7,** 95–99
41. Dougherty, D. A. (1996) *Science* **271,** 163–168
42. Ma, J. C., and Dougherty, D. A. (1997) *Chem. Rev.* **97,** 1303–1324
43. Li, A. J., and Nussinov, R. (1998) *Proteins* **32,** 111–127
44. Smit, A. B., Celie, P. H., Kasheverov, I. E., Mordvintsev, D. Y., van Nierop, P., Bertrand, D., Tsetlin, V., and Sixma, T. K. (2006) *J. Mol. Neurosci.* **30,** 9–10
45. Celie, P. H. N., van Rossum-Fikkert, S. E., van Dijk, W. J., Brejc, K., Smit, A. B., and Sixma, T. K. (2004) *Neuron* **41,** 907–914
46. Ames, G. F., Liu, C. E., Joshi, A. K., and Nikaido, K. (1996) *J. Biol. Chem.* **271,** 14264–14270
47. Davidson, A. L., Shuman, H. A., and Nikaido, H. (1992) *Proc. Natl. Acad. Sci. U. S. A.* **89,** 2360–2364
48. Horn, C., Bremer, E., and Schmitt, L. (2005) *FEBS Lett.* **579,** 5765–5768
49. Bohl, E., Shuman, H. A., and Boos, W. (1995) *J. Theor. Biol.* **172,** 83–94
50. Merino, G., Boos, W., Shuman, H. A., and Bohl, E. (1995) *J. Theor. Biol.* **177,** 171–179
51. Telmer, P. G., and Shilton, B. H. (2003) *J. Biol. Chem.* **278,** 34555–34567
52. Tang, C., Schwieters, C. D., and Clore, G. M. (2007) *Nature* **449,** 1078–1082
53. Millet, O., Hudson, R. P., and Kay, L. E. (2003) *Proc. Natl. Acad. Sci. U. S. A.* **100,** 12700–12705
54. Kempf, B., Gade, J., and Bremer, E. (1997) *J. Bacteriol.* **179,** 6213–6220
55. Padilla, J. E., and Yeates, T. O. (2003) *Acta Crystallogr. Sect. D Biol. Crystallogr.* **59,** 1124–1130